Journal of Korean Society of
Coastal and Ocean Engineers
Vol. 17, No. 4, pp. 259~268, December 2005

Effects of Ocean Outfall for Elimination of the Anoxic Layer in Youngsan River Estuary

영산강 하구언에서 저 산소 층의 제거를 위한 해양방류구의 효과

Seok Jae Kwon, Yang Ki Cho and Il Won Seo*

권석재* · 조양기** · 서일원*

Abstract : There has been a growing interest in the elimination of anoxic layer in the Youngsan River Estuary because the anoxic water mass caused mainly by the inflow of fresh water from the sea wall might cause the mass reduction of benthos during summer. An ocean outfall system to discharge treated wastewater into sea water may be used as one of the effective and economical ways to eliminate the anoxic layer. The suitable ocean outfall design is generally proposed for the prediction of the buoyant jet behavior in the near field. The parameters including CTD and current data are taken into account for more reliable buoyant jet behavior calculation. One of the numerical models, CORMIX 1, approved by EPA is used herein for the prediction of the trajectorial variation of the cross-sectional salinity and DO concentration distribution on the calculated buoyant jet boundary according to the tidal periods. On the basis of the results, it is suggested that the single port outfall is a useful system to eliminate the anoxic layer. Proper strategies are also proposed for achieving desirable ambient conditions.

Keywords : anoxic layer, Youngsan River Estuary, ocean outfall, CORMIX 1, DO

요 지 : 여름에 기본적으로 방조제 내부로부터 담수의 유입으로 발생된 저 산소 수괴가 저서생물의 감소를 야기 시키기 때문에 영산강 하구언에서 저 산소층의 제거에 대한 관심이 증폭되어왔다. 처리된 하 · 폐수를 해양에 방류하는 해양방류시스템이 이러한 저 산소층을 제거하는 효율적이고 경제적인 방법으로 이용되어 질 수 있다. 본 연구에서는 근역에서 방류된 부력제트의 거동을 예측하고자 적절한 방류구의 설계가 제안되었다. 신뢰할 수 있는 부력제트의 거동에 대한 계산을 수행하기 위하여 측정된 CTD와 해류 자료 등을 포함한 인자들이 고려되어졌다. 조석의 주기에 따라 계산된 부력제트의 경계 내에 염분도와 용존산소의 횡분포의 변화를 예측하고자 여러 수치모형중의 하나로 EPA에 의해 승인된 CORMIX 1 모형을 사용하였다. 수치실험의 결과를 기준으로 볼 때 단공방류구가 저 산소층을 제거하는데 유용한 시스템임을 알 수 있었다. 원활한 주변수의 조건을 만족시키기 위하여 적절한 전략이 또한 제안되어졌다.

핵심용어 : 저 산소층, 영상강하구언, 해양방류구, CORMIX 1, 용존산소

1. INTRODUCTION

Reclamation project led to the construction of the sea wall in the Youngsan River estuary as shown in Fig. 1 as the Youngsan River has been one of the five major rivers in South Korea. However, the construction of the sea walls resulted in the very weak tidal currents in the estuary and led to the significant reduction of the vertical mixing. The estuary was then stratified due to weak tidal currents, strong solar radiation, and large fresh water inflow in especially summer. Moreover, the huge quantity of dissolved oxygen is consumed because the particle-organic substances

*서울대학교 지구환경시스템공학부(Corresponding Author: Seok Jae Kwon, Division of Civil, Urban & Geosystem Engineering, Seoul National University, San 56-1, Shinlim-dong, Gwanak-gu, Seoul 151-742, Korea. sj79kwon@chol.com)
**전남대학교 지구환경과학부(Faculty of Earth Systems and Environmental Science, Chonnam National University, Kwangju 500-757, Korea)

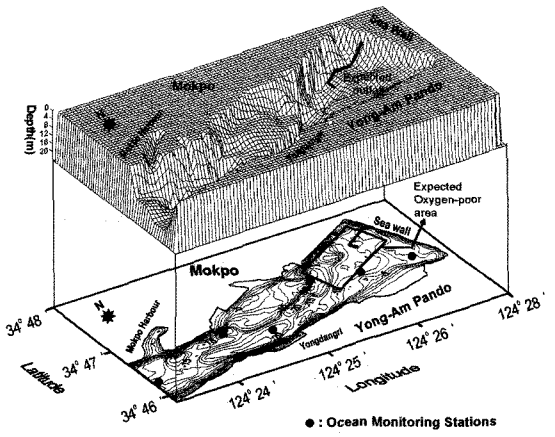

Fig. 1. Bathymetry, proposed outfall, and ocean monitoring stations in the Youngsan river estuary.

are accumulated in the bottom layer. Therefore, the huge anoxic water mass was formed in the bottom layer in the Youngsan River estuary. This anoxic layer has caused the mass reduction of benthos (Lim and Park, 1998). The proposed outfall and estuary topography are shown in three-dimensional bathymetry in Fig. 1.

A number of ocean outfalls over the world discharge primary treated effluent into deep water for efficient wastewater treatment (Fischer et al., 1979; Kang et al., 2000; Seo and Yeo, 2002). An ocean outfall may be used as one of the effective ways to eliminate the anoxic layer. Therefore, in this study, the general outfall with simple single pipe is designed and proposed to remove the anoxic layer through literature search (Grace, 1978; Roberts, 1990). In this study, the discharge system with the single port at the end of the pipe connected from inner side of the bank through the sea wall to the bottom of the estuary is proposed. This discharge system in the Youngsan River Estuary may force the enough anoxic water mass to the surface due to the fast initial velocity of the sufficient effluent (Fig. 2). It is expected that the buoyant jet facilitate the destruction of the mixing layer leading to the restriction of the vertical mixing as well as the increase of DO concentration in the anoxic layer. On the basis of the results, proper strategies will be described in especially summer.

Buoyant effluent discharged from the submerged single-port is initially attached to the bottom and entrained by the ambient water. The effluent then begins to rise as shown in Fig. 2. The plume stops rising at a level of neutral buoyancy, known as the "established field". The region where mixing is caused by the turbulence generated by effluent momentum and buoyancy, is also known as "near field". The dilution in the near field results from the entrainment caused by the combined effects of the momentum and buoyancy of the effluent, and turbulent mixing near the port. Dilution can be defined as the ratio of the initial concentration to the concentration at a certain point of the buoyant jet. The established plume then drifts with the ocean current and is diffused by oceanic turbulence in a region called "far field" (Baumgartner et al., 1994).

The CORMIX (Cornell Mixing Zone Expert System) model approved by EPA(Environmental Protection Agency) has been used in this study for the prediction of the salinity and DO(dissolved oxygen) distribution. The parameters include CTD(conductivity, temperature, and depth) profile, flow rate, number of ports, port angle, port depth, effluent DO and salinity, Ambient DO and salinity, port diameter, current direction, and current speed that are inputted in the model for the description of jet and plume behavior (Jirka et al., 1996). The density profiles can be calculated from

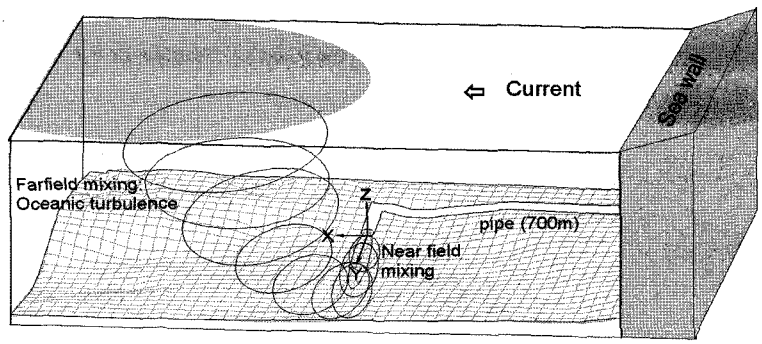

Fig. 2. Schematic description of the buoyant jet discharged from the submerged single port.

the salinity and temperature profiles. The flow rates can be also estimated according to the tidal periods from the application of one dimensional energy equation. The variations of salinity and DO concentration after the effluent will be described. The vertical DO and salinity profiles from the CTD profiles around the anoxic area are almost homeogenous below the mixing layer in summer. The general buoyant jet boundaries can be also predicted according to the tidal periods during summer.

2. PROPOSED OUTFALL

In this study, it is proposed that the pipe is connected from the inlet inside the bank through the sea wall to the bottom in the Youngsan River Estuary to discharge fresh water reserved in the bank into the bottom where the anoxic water mass is dominant (Fig. 3(a)). The details of the pipe are not described because this study does not provide the construction of the ocean outfall but the possibility of the outfall to facilitate the increase of the DO concentration in the anoxic layer. This outfall system is not assumed to consist of pump and turbine.

The multiport diffuser at the end of single pipe has been used to discharge treated wastewater into sea water in many countries so far. However, the main purpose to propose the outfall around this anoxic area where the DO concentration is only about 1 mg/l below mixing layer during summer is to maximize the DO concentration providing the oxygen-rich fresh water into the anoxic layer. The multiport diffuser having small diameters of the ports may not be effective in this case since low discharge in each port may lead to the reduction of the jet volume and DO concentration below the mixing layer (Kwon and Lee, 1997). In this study, the multipipe system is not considered due to the consideration of economical construction costs.

Among the many kinds of pipe material, steel pipes have been widely used in the numerous outfall and are also cheap and easy to construct and transport. A protective anti-corrosion coating is applied to the outside and inside of the steel pipe. In this study, 2 m of pipe diameter is selected for the necessity of huge discharge to sweep the anoxic layer. Therefore, the steel is economically and practically suitable, and reliable for the material of the pipe on the sea bed.

The depth of the outfall is chosen as 10 m. The bottom near the outfall is assumed to be flat because the bottom around the outfall shows the 10 m depth contour line horizontal to the sideline of the sea wall seems to be stable and somewhat flat as shown in Fig. 1. The DO concentration was measured to be extremely low around the outfall (Lim and Park, 1998). The length of the pipe, approximately 700 m, can be fitted to the bottom topography (Fig. 1). The pipe

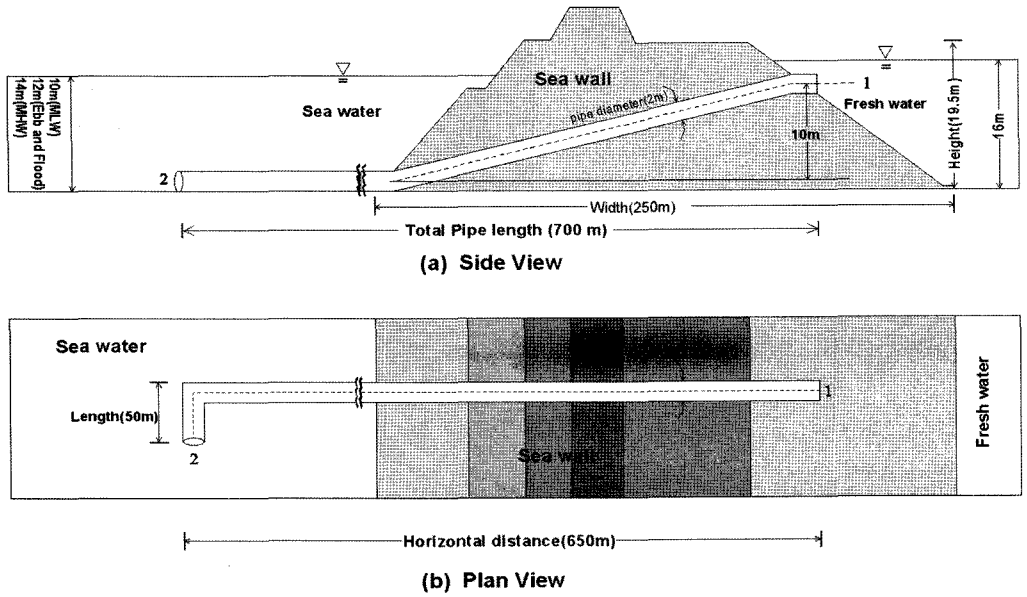

Fig. 3. Plan view and side view of the proposed ocean outfall.

is intentionally bent near the 10 m depth contour line to increase the area covered by the buoyant jet bent by the cross flows of the main tidal currents (Fig. 3(b)).

There are also the possible configurations of the pipe supported by rocks, strap, anchor, and trench. In real situation, the long wave and strong current-induced water particle movement is so strong that the pipe can be moved and damaged along steep bottom. In this study, the pipe may be possibly stable due to the weak current and short wave-induced horizontal and vertical water particle movement (Grace, 1978). Therefore, in this study, any supporting material is assumed to be unnecessary for the protection of the pipe movement.

3. Numerical Model

3.1 General Description of CORMIX 1

CORMIX (Cornell Mixing Expert System) is a software system for the analysis, prediction, and design of pollutant discharges into diverse water bodies. The CORMIX is a useful model employing length scale analysis and asymptotic solutions to jet and plume flows and concerning a wide range of condition (Roberts, 1995). CORMIX system consists of CORMIX 1 for submerged single port discharges, CORMIX 2 for submerged multiport diffuser discharges, and CORMIX 3 for buoyant surface discharges.

The CORMIX 1 is used herein for the description of the buoyant jet behavior since the CORMIX 1 predicts the boundary and dilution characteristics of the initial mixing zone for submerged single port discharge. In the CORMIX 1 model, the various flow patterns developed by the discharged effluent mixing with the surrounding water does not determine only the boundary, size, and mixing intensity, but also any impact of the plume on water surface, sea bed, or shore line. The various flow types depending on the physical processes in the near field govern effluent discharge mixing. The near field processes including the buoyant jet mixing, added effects of current or density stratification, and plume interaction with any boundaries lose their importance beyond the immediate near field. In this model, the buoyant jet boundary line is defined as the line corresponding to the $1/e$ of the maximum concentrations along the cross-sections normal to the trajectory. The details of the mathematical description and procedure of the flow categories are provided in the User's Manual for CORMIX (Jirka et al., 1996) and hydrodynamic classification of submerged single port discharge (Jirka and Doneker, 1991).

3.2 Input Parameters

3.2.1 Typical Density Profile

The density stratification over the water column has significant impacts on the plume behavior such as rise height and dilution (Roberts, 1995). The density profiles were obtained from the salinity and temperature profiles, which were measured at 6 stations (Fig. 1). Among the calculated density distributions, the density profiles representing summer and winter are shown in Fig. 4. These types of the den-

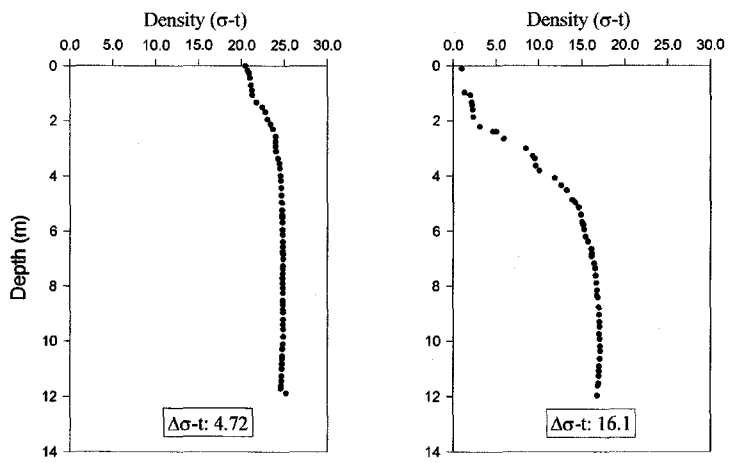

(a) Density Profile (February, 1998) (b) Density Profile (August, 1998)

Fig. 4. Density profiles measured at the nearest station to the proposed outfall in the Youngsan river estuary.

sity profiles are very frequent and typical in real situation. The homogeneous density profile measured in winter is shown over the whole column (Fig. 4(a)). The strong density stratification from the density profile measured during summer may lead to slow plume rise around the level of mixing layer due to the significant density difference between the upper layer and low layer. The stratified density profile (Fig. 4(b)) will be used for the buoyant jet behavior description since this study focuses on the anoxic layer generated during summer.

The density profiles inputted in the CORMIX model covers three types of them: linear density profile, two-layer profile with constant densities and density jump, and constant density surface layer with linear density distribution in bottom layer separated by a density jump (Jirka et al., 1996). To input the non-uniform density profiles to the CORMIX model, a straight line is fitted to the average value in each layer of the density profile.

3.2.2 Flow Rate

The calculation of the flow rate through the pipe is required to predict the buoyant jet behavior as one of the input parameters in the CORMIX model. The side view of the pipe location is shown in Fig. 3. The flow rates can be simply calculated in terms of the pressure difference related to the water level difference between fresh water and sea water. In other words, the flow rates based on the tidal periods (MHW, maximum ebb, MLW, and maximum flood) are calculated and inputted in the CORMIX model as input parameters for achieving the proper strategies.

One dimensional energy equation based on Bernoulli's equation is written from the level of the inflow of fresh water to the free jet,

$$\frac{p_1}{\rho_1 g}+\frac{V_1^2}{2g}+z_1-h_f-h_{lm}=\frac{p_2}{\rho_2 g}+\frac{V_2^2}{2g}+z_2 \quad (1)$$

where p is the pressure (Pa), V is the fluid velocity, is the density of the fluid, g is the gravitational acceleration, z is the elevation at each point, h_f is the major head loss due to frictional effects in fully developed flow in a constant area pipe, and h_{lm} is the minor head loss caused by area change such as entrance, fittings, and bends. It is assumed that there are no heat transfer and internal energy change inside a pipe.

The pressure at 1 and 2 points at different depth is given by $p=p_a+gh$, at which p_a is the standard atmospheric pressure at sea level (101.3 kPa), and h is the water depth at each point. V_1 is assumed to be 0 m/s.

The major head loss can be calculated from the Darcy-Weisbach equation as

$$h_f=f\frac{L}{D}\frac{V_2^2}{2g} \quad (2)$$

where f is the resistance coefficient, L is the length of the pipe, and D is the pipe diameter. The resistance coefficient (f) is calculated from the Moody Diagram as a function of Reynolds Number. The minor head loss can be expressed by

$$h_{lm}=K\frac{V_2^2}{2g} \quad (3)$$

where K, the loss coefficient, includes the values for a pipe entrance (K=0.50), a pipe exit (K=1.00), and a bend (K=0.2) with vanes (Roberson and Crowe, 1993).

The Reynolds Number is given by $Re=V_2D\rho/\mu$, where V_2 is the flow velocity in the pipe, and is the dynamic viscosity. The relative roughness can be expressed as k_s/D, where k_s is the equivalent sand roughness (0.046 mm for steel) based on the material of the pipe. Two unknowns of the values of f and V_2 can be solved from the iteration of the following procedure. The initial value for f is guessed, and the velocity V_2 is then solved (Roberson and Crowe, 1993).

3.2.3 Other Parameters

The port diameter of 2 m is imposed at the depth of 10 m based on MLW. The difference of sea level between MHW and MLW is approximately 4 meters. The centerline of the port is assumed to be horizontal to the bottom plane based on the bathymetry in the vicinity of the outfall. The effluent density is chosen to be 998 kg/m^3 since the approximate physical temperature of fresh water at 20 °C in atmospheric pressure indicates the value of 998 kg/m^3 (Roberson and Crowe, 1993).

It is assumed that the currents around the study area are steady and uniform due to the limitation of the CORMIX 1 model. The dynamics of the initial dilution process of this outfall focuses on the near field below the mixing layer due to significant anoxic water mass. The mixing processes in the near field are quite rapid relative to the time scale of hydrographic variation although the tidal cycle of the actual current has relatively long time scale. Therefore, the buoyant jet behavior analysis can be performed under the

assumption of steady state of ambient water based on the each tidal period (Jirka, 1998). The tidal current directions measured in the vicinity of the outfall was nearly perpendicular to the direction of the discharge. The main tidal current directions point to the offshore for ebb tide and to the sea wall for flood tide. The amplitude of the tidal currents measured near the expected outfall is approximately 0.2 m/s (Lee, 1994).

Actually, the vertical DO concentration distribution and salinity profile are evidently nonuniform. It is observed that the salinity profiles taken from the CTD data are almost homeogenous below the stratification whereas the salinity values are quite low in the upper layer due to the fresh water discharged through water gates. It is also expected that the DO concentrations are almost uniform and quite low below the mixing layer whereas the range of the DO concentrations is 8.0 to 9.0 mg/l in the upper layer (Lee, 1994). The average observed values of 25.7 ‰ for salinity and 1 mg/l for DO concentration below the mixing layer in summer are inputted into CORMIX 1 model since the CORMIX model allow only uniformity of ambient concentration. Therefore, the concentration distribution predicted by CORMIX 1 model below the mixing layer will be provided and concerned for the interests of anoxic layer below the mixing layer.

4. NUMERICAL RESULTS

4.1 DO Concentration Distribution

The buoyant jet behavior predictions for the proposed outfall have been performed by CORMIX 1. The cross-sectional and trajectorial distributions of DO concentration and salinity below the mixing layer, and the buoyant jet boundary in the near field were predicted according to the tidal periods for especially summer. The location of the origin is the bottom point of the single port at the end of pipe. The x-axis indicates the horizontal Cartesian coordinate to the offshore; the y-axis indicates the horizontal Cartesian coordinate to the jet direction; and the z axis points vertically upward (Fig. 2).

All of the buoyant jet flows in the given conditions for 4 tidal levels was classified as 'H4-90A4' representing the buoyant flows attached to the bottom on the range of dominant effluent momentum. In Fig. 5, the variations of cross-sectional and trajectorial DO concentration below the pycnoline are shown in the plan view and side view of the predicted buoyant jet geometry in the near field for the maximum ebb tide. In this figure, the reduction of the jet width along the trajectory occurs in the range between 19 m and 25.5 m on the y-axis because the pressure gradient results from the effluent momentum transported to the ambient water. The zone between C-C' and D-D' can be divided into 2 categories: the acceleration zone (gradual reduction zone) due to the increase of flow velocity and the diffusion zone. This flow is called 'contracting slipstream', which is shown in all jet flows predicted for 4 tidal levels (Lee and Seo, 1996).

It is seen that the maximum concentrations attached to the bottom up to the horizontal distance 26 m on the y-axis due to the somewhat strong effluent momentum. The Gaussian profiles along the selected cross-sections in the buoyant jet were assumed in the CORMIX model and verified by many researchers (e.g., Papanicolaou, 1984; Hongwei, 2000). The plume then begins to rise after the distance of 26 m because the buoyancy effect begins to gradually increase relative to the effluent momentum. Therefore, the maximum concentration on the bottom begins to move to the center of the cross-section normal to trajectory after the rise of the buoyant jet. The attachment of the buoyant jet to the mixing layer occurs at the horizontal distance 38.8 m (the end of near field, established field) on the y-axis.

The concentrations along the centerline trajectory decrease due to the mixing with the ambient water. However, the centerline concentration in the section of C-C' is observed to be identical to that in the section of D-D' in the contracting slipstream zone since the centerline concentrations are nearly constant in the contracting slipstream zone due to the dominant advection generated in the acceleration zone. The maximum DO concentrations higher than 3.9 mg/l in the anoxic layer for all tidal periods seem to be sufficient to satisfy the desirable DO condition.

In Fig. 5, it is seen that the centerline of the trajectory is somewhat bent to the offshore due to the direction of maximum currents in the near field. The Gaussian profiles of the DO concentration along the chosen cross-sections in the jet show the symmetric distributions with respect to the centerline near the mixing layer. The boundaries and DO concentration distributions of the buoyant jet predicted for the maximum flood tide are evidently symmetric to those for the maximum ebb tide on the plan view with respect to the y-axis due to the only current direction (to the sea wall)

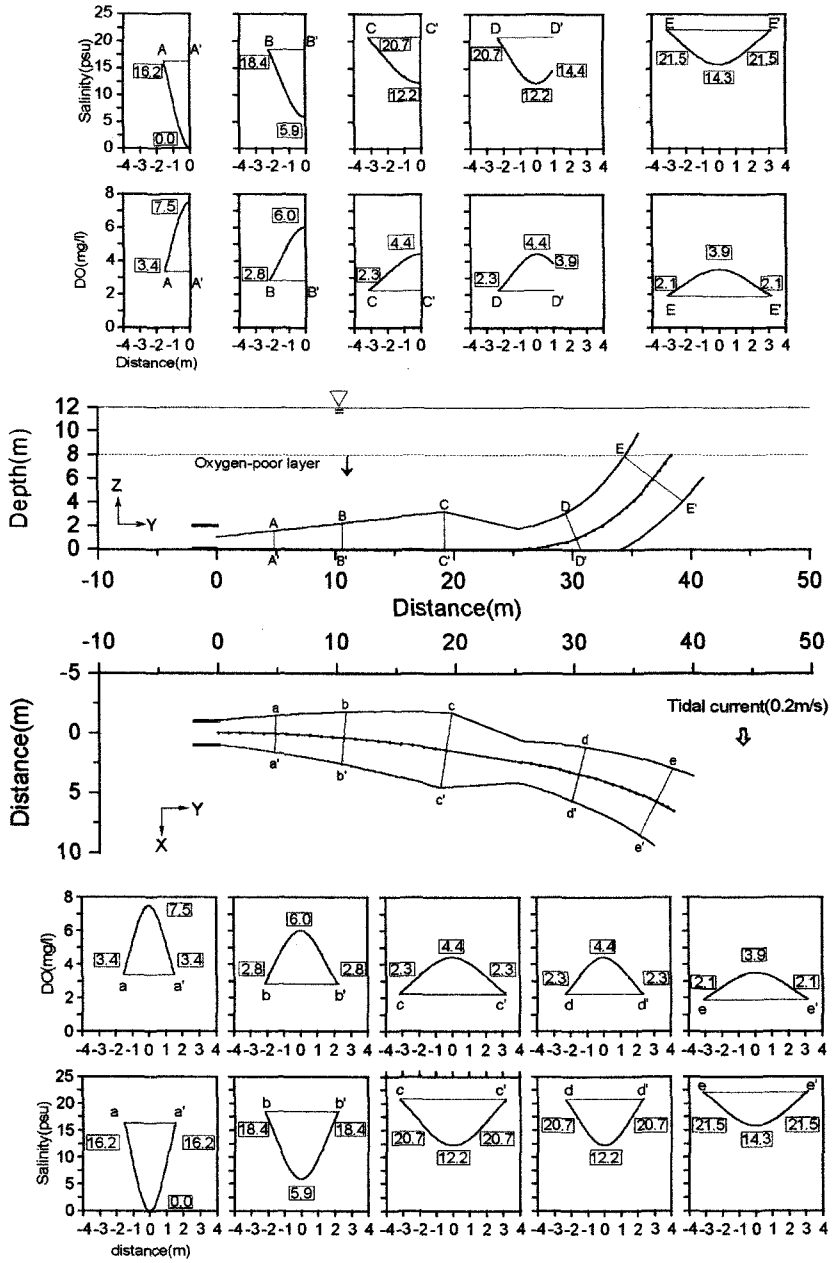

Fig. 5. Side view and plan view of the predicted variation of the cross-sectional DO concentration and salinity distribution in the buoyant jet boundary for maximum ebb tide.

opposite to that for the maximum ebb tide under the same flow rates and same current magnitudes.

The maximum concentration for MHW is attached on the bottom up to the horizontal distance of 17 m (on the y-axis), which is relatively lower than the value, 26 m, for the maximum ebb tide due to the low effluent momentum caused by the low flow rate. The centerline of the trajectory for the MHW and MLW lies on the y-axis on the plan view due to the stagnant ambient condition. The maximum concentration for MLW is attached on the bottom up to the horizontal distance of 32 m (on the y-axis), which is relatively higher than the value of 26 m for the maximum ebb tide due to the

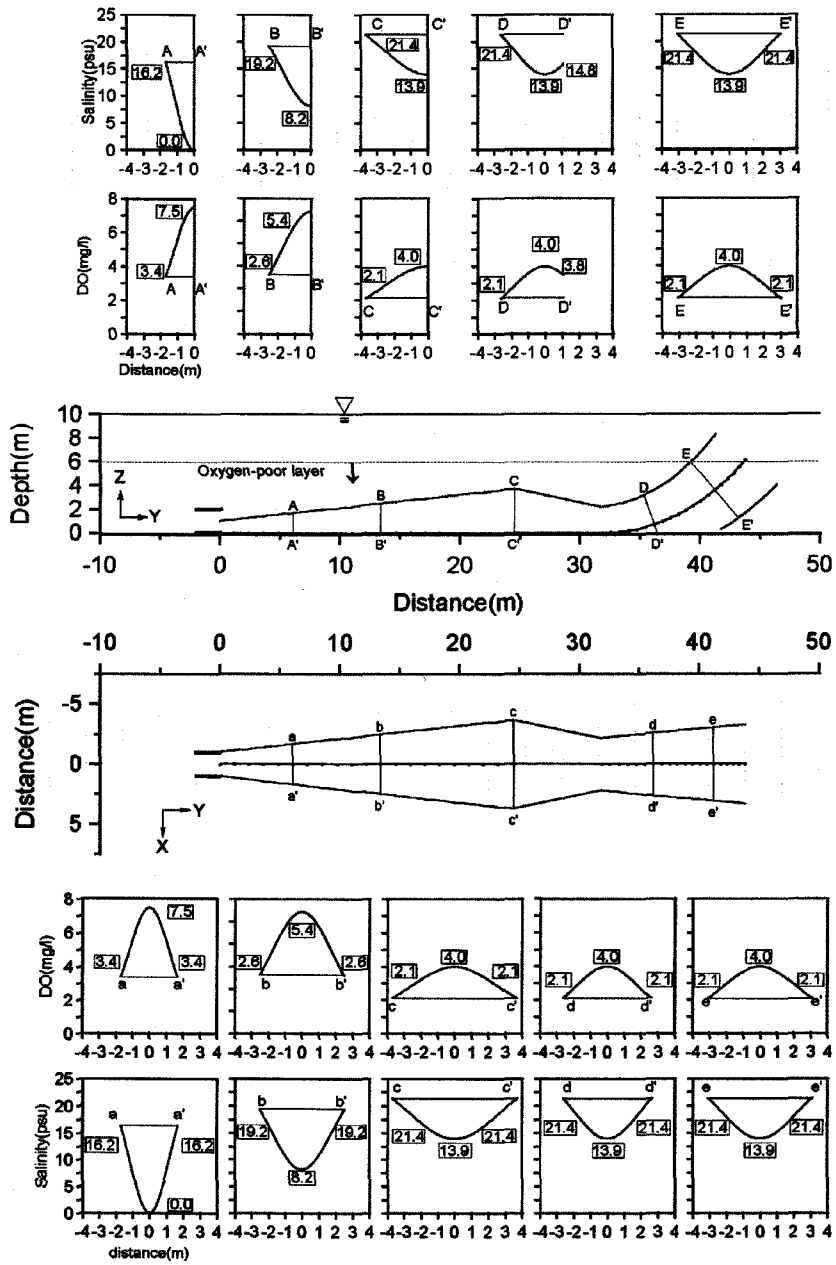

Fig. 6. Side view and plan view of the predicted variation of the cross-sectional DO concentration and salinity distribution in the buoyant jet boundary for MLW.

high effluent momentum resulting from the big pressure difference as shown in Fig. 3 (Fig. 6). The numerical results for DO shows that the fresh effluents during the MLW, ebb, and flood may be more effective and proper strategies than those for the MLW due to the high flow rates and the buoyant jets bent to the offshore and sea wall.

4.2 Salinity Distribution

The variations of salinity distribution in the chosen cross-sections below the pycnoline are shown on the plan view and side view of the predicted buoyant jet in the near field for the maximum ebb tide and MLW (Fig. 5 and 6). On the contrary to the Gaussian profiles for the DO concentration,

the minimum concentration lies on the bottom initially since the effluent of fresh water is discharged to the saline ambient water with the salinity of 25.7 ‰ (Fig. 5 and 6). The profiles of the salinity along the chosen cross-sections in the buoyant jet also shows the symmetric distributions on the plan views with respect to the centerline. The maximum values among the minimum salinity values along the trajectory below the stratification are observed to be 8.4, 14.3, and 14.4 psu, respectively, for the MHW, maximum ebb (or maximum flood), and MLW.

5. CONCLUSIONS

The prediction of the behavior of the buoyant jet discharged from the given single port was made by the CORMIX 1 model according to the tidal periods to determine the effects of the outfall on the elimination of the anoxic layer. Among the density distributions measured at six stations in Youngsan river estuary, the stratified density profile for summer was used for the buoyant jet behavior calculation. The flow rates were simply estimated according to the tidal periods (MHW, maximum ebb, MLW, and maximum flood) using the one dimensional energy equation based on Bernoulli's equation. The other parameters such as the depth, currents, port angle, port diameter, effluent conditions, and ambient conditions were also inputted into the CORMIX 1 model with the consideration of the tidal periods. The dynamics of the initial dilution process of this outfall focused on the near field below the mixing layer due to significant anoxic water mass.

All of the buoyant jet flows in the given conditions for 4 tidal levels was classified as 'H4-90A4' indicating the buoyant flows attached to the bottom on the range of dominant effluent momentum. The maximum concentrations were initially attached to the sea bed up to the horizontal distances of 17 m, 26 m, and 32 m for the MHW, maximum ebb (or maximum flood), and MLW, respectively. The reduction of the jet width along the trajectory was observed due to the dominant advection generated in the acceleration zone and was called 'contracting slipstream' where the centerline concentrations were nearly constant. The maximum DO concentrations in each cross-section for the all tidal periods range from 3.9 to 7.5 mg/l in the buoyant jet in the anoxic layer. The maximum values among the minimum salinity values along the trajectory below the stratification were observed to be 8.4, 14.3, and 14.4 psu, respectively, for the MHW, maximum ebb (or maximum flood), and MLW.

The buoyant jet seems to result in the destruction of the stratification and then makes the vertical mixing active. The jet flow supplies directly the oxygen-rich water from the river to the oxygen poor layer. The sea water with rich oxygen in the upper layer might provide additional oxygen to the bottom layer by vertical mixing. In order to maximize the effects on the elimination of the oxygen poor layer, the fresh effluents for the MLW, ebb, and flood can be more effective strategies than those for the MLW due to the high flow rates and the buoyant jets bent to the offshore and sea wall.

ACKNOWLEDGEMENT

Data collection was supported by the Korean Research Foundation (1988-022-H00008). A post-doctoral researcher in the Mokpo National Maritime University, Yong Woo Park, provided useful information which are gratefully appreciated.

REFERENCES

Baumgartner, D.J., Frick, W.E. and Roberts, P.J.W. (1994). Dilution models for effluent discharge. U.S. Environmental Protection Agency, Office of Research and Development, Washington DC.

Fischer, H.B., List, E.J., Koh, R.C.Y., Imberger, J. and Brooks, N.H. (1979). Mixing in Inland and Coastal Waters. Academic Press, New York.

Grace, R.A. (1978). Marine Outfall Systems (Planning, Design, and Construction). Presentice-Hall, New Jersey.

Hongwei, W. (2000). Investigations of buoyant jet discharges using digital particle velocimetry (DPIV) and planar laser induced fluorescence (DPIV). Ph.D. thesis, School of Civil and Structural Engineering, Nanyang Technological University, Singapore.

Jirka, G.H. (1998). Mixing processes and buoyant jet theory. Institute for Hydromechanics, University of Karlsruhe, Karlsruhe, Germany.

Jirka, G.H., Doneker, R.L. and Hinton, S.W. (1996). User's Manual for CORMIX: A Hydrodynamic Mixing Zone Model and Decision Support System for Pollutant Discharges into Surface Waters. School of Civil and Environmental Engineering, Cornell University, New York.

Jirka, G.H. and Doneker, R.L. (1991). Hydrodynamic classification of submerged single-port discharges. Journal of Hydrau-

lic Engineering, ASCE, 117(9), 1095-1112.

Kang, S.W., You, S.H. and Na, J.Y. (2000). Near-field mixing characteristics of submerged effluent discharge into Masan Bay. Ocean Research, 22(1), 45-56

Kwon, S.J. and Lee, J.W. (1997). Plume rise and initial dilution determination reflecting the density profile over entire water column. The Korean Institute of Port Research, 11(2), 215-230.

Lee, J.H. and Seo, I.W. (1996). Predicting mixing characteristics of heated-water discharged by submerged multi-port diffuser. Journal of Korean Society of Civil Engineers, 16(3), 281-290 (in Korean).

Lee, S.W. (1994). Korean Harbor Hydraulics. Jipmoondang Company, Seoul, Korea.

Lim, H.S. and Park, K.Y. (1998). Community structure of the macrobenthos in the soft bottom of Youngsan river estuary, Korea. The Korean Fisheries Society, 31, 330-342

Papanicolaou, P.N. (1984). Mass and momentum transport in a turbulent buoyant vertical axisymmetric jet. Ph.D. Thesis, California Institute of Technology, USA.

Roberson, J.A. and Crowe, T.C. (1993). Engineering Fluid Mechanics (Fifth Edition). Houghton Mifflin Company, Boston and Toronto.

Roberts, P.J.W. (1990). Outfall Design Considerations. The Sea, Ocean Engineering science. Wiley Interscience, New York.

Roberts, P.J.W. (1995). Plume modeling. Mamala Bay Study, Report No. Project MB-4, 1, Mamala Bay Study Commission, City and County of Honolulu, Honolulu.

Seo, I. W. and Yeo, H. K. (2002) Near-field dilution of Rosette type multiport wastewater diffusers. Water Engineering Research, 3(2), 93-111.

Received July 28, 2005

Accepted December 5, 2005